A Spatial Hypergraph Model Where Epidemic Spread Demonstrates Clear Higher-Order Effects

Omar Eldaghar[1(✉)], Yu Zhu[2], and David F. Gleich[2(✉)]

[1] Department of Mathematics, Purdue University, West Lafayette, IN, USA
oeldagha@purdue.edu
[2] Department of Computer Science, Purdue University, West Lafayette, IN, USA
{zhu1246,dgleich}@purdue.edu

Abstract. We demonstrate a spatial hypergraph model that allows us to vary the amount of higher-order structure in the generated hypergraph. Specifically, we can vary from a model that is a pure pairwise graph into a model that is almost a pure hypergraph. We use this spatial hypergraph model to study higher-order effects in epidemic spread. We use a susceptible-infected-recovered-susceptible (SIRS) epidemic model designed to mimic the spread of an airborne pathogen. We study three types of airborne effects that emulate airborne dilution effects. For the scenario of linear dilution, which roughly corresponds to constant ventilation per person as required in many building codes, we see essentially no impact from introducing small hyperedges up to size 15 whereas we do see effects when the hyperedge set is dominated by large hyperedges. Specifically, we track the mean infections after the SIRS epidemic has run for a while so it is in a "steady state" and find the mean is higher in the large hyperedge regime whereas it is unchanged from pairwise to small hyperedge regime.

Keywords: hypergraphs · epidemic spread · higher-order epidemics · spatial hypergraph model · SIRS epidemic

1 Introduction

One of the key questions regarding epidemic spread on higher-order graph models is whether the higher-order structure is relevant to macroscopic properties of the epidemic. On the one hand, epidemic spread is *inherently* a pairwise behavior in which a real or virtual pathogen spreads from one individual to another in an infection event. On the other hand, pathogens spread via airborne routes have obvious group-relevant interactions [18]. Theoretical and empirical studies on these findings have been mixed. As shown by [15], without strong hyperedge-dependent infection effects, hyperedge transmission models reduce to weighted pairwise transmission models. Studies of human mobility and SARS-CoV-2 showed that super-spreading and the associated group interactions were key

H. Cherifi et al. (Eds.): COMPLEX NETWORKS 2024, SCI 1188, pp. 43–55, 2025.
https://doi.org/10.1007/978-3-031-82431-9_4

routes of transmissions [9,11]. However, there are issues with each of these procedures. Theoretical models often assume probabilistic epidemics that smooth out behaviors; empirical data tend to be a messy mixture of multiple different processes. Suffice it to say, studying epidemics is challenging with multiple tradeoffs among approaches [1]. Put plainly, we wished to understand if there is an easy-to-understand scenario where hypergraph epidemic spreading was relevant in order to assist in future studies of more fine-grained behavior and mechanisms.

In this paper, we seek to study epidemic processes in an idealized case to demonstrate the magnitude of the possible difference in epidemic behavior in the light of group structure on hypergraphs. This is important because our findings will shed light on what types of differences distinguish pairwise spread from hypergraph spread. To make our findings concrete, we will adopt a simple spatial hypergraph model – which we will discuss in future sections – that incorporates degree heterogeneity as well as local clustering, both key properties of empirically observed human behavior. The model works by running a *clustering* algorithm on the nearest neighbors for each node. Each cluster becomes a hyperedge. By varying a parameter of the clustering algorithm, we can interpolate between purely pairwise edges (putting each neighbor into a single cluster) and entire hyperedges (one cluster for the entire neighborhood). We divide this parameter space into two regions, one that interpolates from pairwise edges to small hyperedges and another that interpolates from small hyperedges to big hyperedges.

We study these networks with a discrete-time susceptible-infected-recovered-susceptible (SIRS) epidemic model that has been extended to account for spreading in hypergraphs. Specifically, the hypergraph extension is designed to model airborne spread and also incorporate airborne dilution effects. Our idea is that the study of hypergraph spread corresponds to a hypergraph model where the hyperedges represent a *group interaction*, and so bigger groups must meet in larger areas or areas with additional ventilation (which is typically specified per person in many building codes). Since this is a SIRS epidemic, there is an initial *spike* in infections in the entirely susceptible population. Following this spike, and some additional transients, the behavior enters a "steady state" where infections per time step are roughly constant. We use the average behavior in this steady state as a proxy for a relevant epidemic property that is macroscopically evident.

We find that these SIRS epidemics show a clear impact in the big hyperedge regime. In particular, the mean average infections over the last period of epidemic simulation is higher for big hyperedges (Fig. 5). This finding holds even though the total epidemic forcing due to edges in a pairwise projected model of the hypergraph epidemic is constant and the spectral epidemic growth factor λ_1 of the pairwise projected model is constant or lower. Consequently, these demonstrate the scenario we sought: a simple scenario that nonetheless causes a macroscopically relevant impact.

2 Preliminaries on Graphs and Hypergraphs

To evaluate the impact of higher-order structures on epidemic spread, we consider models of both graphs and hypergraphs. As mentioned in the introduction, we will introduce a model in the next section that allows us to smoothly interpolate between a purely pairwise graph and a hypergraph in a natural fashion. To that end, we briefly review the notation for graphs and hypergraphs.

An undirected graph $G = (V, E)$ consists of a set of vertices V and a set of edges E, where each edge $e \in E$ connects two vertices from V. The degree of a vertex $v \in V$ is defined as the number of edges incident to it. We allow repeated edges to exist as well. A hypergraph $H = (V, E)$ extends this concept, where V remains a vertex set and now the set E is a hyperedge set. A hyperedge, unlike a standard edge, may connect more than two vertices. The degree of a vertex in a hypergraph is typically defined as the number of hyperedges that contain it.

The projected graph of a hypergraph, obtained through clique expansion, is a pairwise graph in which each hyperedge is replaced by a clique of fully connected vertices (we do not include self-edges). When computing clique expansions, we may sometimes wish to weight the expansion such that the total weight of each hyperedge is bounded. In this case, when we compute the clique expansion, we associate each edge of the clique with a weight $w(e)$ and treat repeated edges from multiple cliques as distinct. There is a relationship between weighted projected graphs and the fractional degrees of a hypergraph [16].

3 The Spatial Hypergraph Model

We propose a new random spatial hypergraph model in a fashion that allows us to easily interpolate among multiple possible graph to hypergraph realizations. The idea is that we have a set of points in space that represent the vertices. Vertices connect up to nearby vertices in a nearest neighbor fashion. We induce hypergraph and group structure by *clustering* the regions of nearby vertices.

Suppose there are n vertices. Each vertex v is associated with a d-dimensional vector x_v and a positive scalar parameter r_v, both of which are randomly generated. The vector x_v indicates the position of vertex v. A straightforward way to generate these coordinate vectors is to distribute n vertices uniformly at random within the unit hypercube $[0, 1]^d$. In this study, we focus on $d = 2$ and position each vertex within the unit square, although the model can be easily generalized to higher dimensions or arbitrary point placements. To mitigate border effects, one could use a wrap-around or hyper torus distance in this space [6,7,12]. Using alternative point distributions would also work. The parameter r_v should be understood as the range of activity of vertex v and directly corresponds to the *number of neighbors* that a vertex will have in the network. This reflects the *social power* or *exposure* range of a given vertex. These values are randomly sampled from a predefined probability distribution; we use log-normal distributions.

To construct hyperedges, we proceed as follows. For each vertex v, we first find its $k_v = \min\{\text{ceil}(r_v), n - 1\}$ nearest neighboring vertices (the adjustments

to r_v guarantee we get an integer that isn't too large). If $k_v = 1$, we add an edge between v and its closest vertex. If $k_v > 1$, we apply the DBSCAN algorithm [13] to these k_v vertices to detect local clusters around v. For each local cluster identified, we add a hyperedge that includes v and the vertices in that cluster.

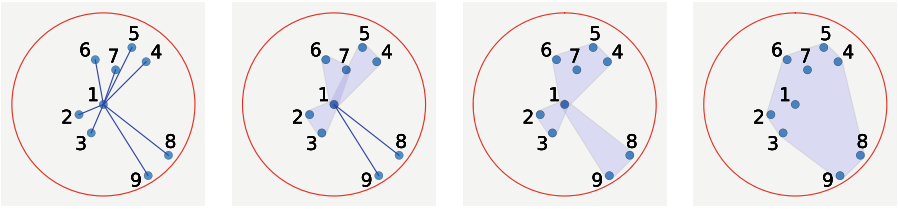

Fig. 1. Hyperedges formed around vertex $v = 1$ with increasing neighborhood radius parameter in DBSCAN (left to right), where $k_v = 8$ nearest neighboring vertices (within the red circle) are considered. Pairwise links form at a small parameter (leftmost), transitioning to a single large hyperedge at a larger parameter (rightmost), with intermediate stages shown in between.

The proposed hypergraph model enables an interpolation between nearest neighbor graphs and hypergraphs whose projections yield nearest neighbor graphs via the neighborhood radius parameter ε (notice that this is different from r_v introduced above) in the DBSCAN algorithm. An illustration is provided in Fig. 1. When this parameter is set very small, each vertex v treats its surrounding k_v vertices as separate clusters, forming k_v simple pairwise edges. This results in a simple nearest neighbor graph. Conversely, a large neighborhood radius merges all k_v vertices into a single cluster, generating one hyperedge connecting v to all its k_v neighbors.

We note that any other clustering method would work here as well, our choice of DBSCAN is because it mirrors our intuition about spatially proximity interactions: groups of nearby points should be connected together into a hyperedge. Also, using a distance parameter avoids directly choosing a number of clusters as in k-means, which is slightly easier to reason about in this model. The reason we like this model for understanding epidemic behavior is that the number of neighbors k_v is independent of the group structure. This allows us to vary the neighborhood radius parameter as a proxy for the strength of group interactions. One challenge here is to normalize this region by the total activity of a node, which we discuss in Sect. 3.1.

Flexibility Within the Model. We conclude by noting that this is a fairly flexible and customizable model. In the interest of space, we do not explore many of these ideas, but wish to mention them for others. (1) Vertex positions can be randomly sampled from bounded regions with various shapes, such as disks or spheres, using different probability distributions. Alternatively, vertex placement can follow population distributions observed in real-world datasets. (2)

The model parameters $\{r_v\}$ can be drawn from distributions other than the log-normal. (3) As mentioned earlier, the neighborhood radius parameter in the DBSCAN algorithm can be tuned to influence the hyperedge formation process, thereby affecting the resulting hyperedge sizes. Other clustering methods can also be considered. (4) In addition, we can introduce a probability parameter p to control whether every hyperedge generated by the model is kept or rejected: with probability p, a hyperedge is kept; otherwise, it is rejected. This introduces more randomness to the model and allows for control over the hyperedge density in the final hypergraph. (5) Also, the distance functions used for computing nearest neighbors can be customized.

3.1 Varying Between Pairwise and Higher-Order Effects

The goal of this paper is to study this model from the perspective of demonstrating higher-order impacts. Consequently, we wanted a simple way to interpolate between small clusters and large clusters. As we alluded to, there's a challenge here because each node has a different choice of k_v. This choice corresponds to a distinct region of space for the nearest neighbors. Fixing a single value of ε for all nodes would work, but would not let them adapt to being randomly assigned to less dense regions of the network. This scenario is illustrated in Fig. 2.

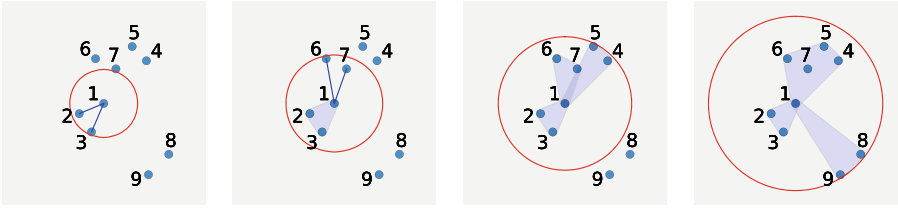

Fig. 2. Hyperedges formed around vertex $v = 1$ as the number of nearest neighbors k_v considered increases (left to right). We want the neighborhood radius parameter in DBSCAN to adjust with k_v and influencing the hyperedge formation. Note that in each case we pick two or three hyperedges. In our experiments, we use ε_α to control this behavior.

In this paper, we then want the neighborhood radius parameter in DBSCAN to scale with the number of nearest neighbors k_v as well as the actual distance from the node to those neighbors. We then let $d_v^{\max}$ denote the maximum distance from v to its k_v nearest neighbors. To combine the two, we use the following function

$$\varepsilon_\alpha(d_v^{\max}, k_v) = \begin{cases} \alpha \cdot d_v^{\max}/\sqrt{k_v} & 0 \le \alpha \le 1 \\ d_v^{\max}/\sqrt{k_v} + (\alpha - 1) \cdot (d_v^{\max} - d_v^{\max}/\sqrt{k_v}) & 1 < \alpha \le 2. \end{cases}$$

Note that ε_0 is zero for all values, so this reflects the pairwise case. Likewise, ε_2 is $d_v^{\max}$, so this reflects the case when the entire set of k_v neighbors will correspond

to a single hyperedge. When $\alpha = 1$, we set an intermediate value designed to create about $\sqrt{k_v}$ hyperedges from those k_v points. Specifically, this is the value $d_v^{\max}/\sqrt{k_v}$.

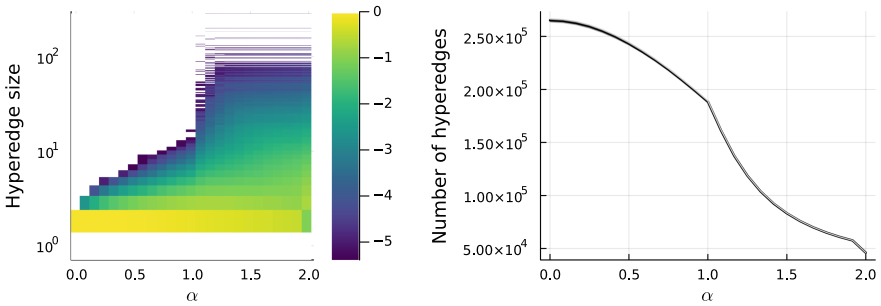

Fig. 3. For a case with $n = 50,000$ vertices that mirrors the experiments in the results section, we show the number of hyperedges and the distribution of hyperedge sizes. This shows that for $\alpha = 1$, we start transitioning from exclusively from pairwise information into small hyperedge data whereas for $\alpha = 2$, there the pairwise data is gone. The reason the number of hyperedges goes down as a function of α is that by making bigger clusters (what α controls in a local fashion) we can only reduce the number of clusters formed, and hence, reduce the number of hyperedges created. Nonetheless, this will keep the projected graph weights constant, see Fig. 6.

We illustrate the impact of α in Fig. 3. This shows how the clusters (i.e. the hyperedge sizes) increase with α whereas the total number of hyperedges decreases with α because they capture the same set of neighboring vertices.

3.2 Related Models

The proposed model draws inspiration from the geometric protean model [7] and its simplified variant [6], among others [23]. We use the idea from these papers that vertices have influence regions of varying sizes, while we go further by considering local clusters within these regions to form hyperedges.

There are several random geometric models in existing work for hypergraphs, as well as for simplicial complexes, which are a special type of hypergraphs with a nested structure (where any subset of a hyperedge is also a hyperedge). One way to generate random geometric hypergraphs is via random geometric bipartite graphs [10], where random points are split into two sets, and edges are formed between vertices from different sets if their distance is within a certain threshold. The two sets can then represent the hypergraph's vertices and hyperedges, respectively. Another approach introduces a radius parameter r_k for each hyperedge size k [23]. For any combination of k vertices, a hyperedge is established if the intersection of their respective r_k-radius balls is non-empty. In general, the radius parameter r_k is set to increase with the hyperedge size k, in order to

generate non-simplicial hypergraphs. When the radius parameters are set equal, the resulting hypergraph is actually a simplicial complex, which is known as the Čech complex. Similar models include the Vietoris-Rips complex and the Alpha complex [4,17,19]. Compared to these models, our proposed model enables an interpolation between geometric graphs and hypergraphs, making it more effective for studying how higher-order interactions affect epidemic processes.

4 The Epidemic Simulation

We model a standard SIRS epidemic simulation. This is a compartmental model with three states: susceptible, infected, and recovered. Nodes represent individuals and they move through these states in order. Recovered nodes represent people who are temporarily immune from infection. A node will move back to susceptible after a sufficiently long time. We study these all with a discrete event simulator that operates on individual time steps. At each time step,

1. with probability β, a susceptible node is infected by an infectious neighbor;
2. with probability γ, a node recovers from infected to recovered;
3. with probability δ, a node transitions from recovered to susceptible

We run this update for each node based on the state of infected nodes at the start of the time step. The expected length of an infection is then $1/\gamma$ and this is binomially distributed. Likewise, the expected length of immunity and recovery is $1/\delta$ and is similarly binomially distributed. The overall epidemic defines a memoryless process over the vector of states for each vertex in the graph.

We also add one more feature, which is a source of exogenous infections. Since the populations we are modeling are small relative to the global population, we want to account for infected nodes arising from outside our small population. Consequently, we add a parameter θ and set a susceptible node to infected with probability θ. Typically, this is very small. For this setup, we view the *graph* or *hypergraph* as a set of contact that the node visits during each time period.

4.1 The Hypergraph Extension

Our goal in modeling a hypergraph epidemic diffusion is to model an airborne infection that would potentially infect a group of contacts. The model we adopt is that each hyperedge represents a *group interaction with shared air*. Consequently, a single infected individual in the hyperedge could infect any other individual in the hyperedge. Note that the only term that needs to be adjusted is the infection.

Our choice for this specific case is that guided by the airborne scenario relevant to group interactions. First, if there are I infected nodes in a hyperedge, then we should model the case of being infected by *any of them*. Second, however, if there are I people in a space, then we assume it has an increased clean air supply [2]. This means that we reduce the chance of infection by a linear fraction. A more accurate model would use the adjusted risk ratios from recent work on airborne spread [20], but our goal is to be simple enough to reason

about without unnecessary complexities. Consequently, the way that we adapt the infection probability is that we change it to $f(\beta, I, m)$, where m denotes the total number of nodes in the hyperedge, I is the total number of infected nodes in the hyperedge, and β is the pairwise infection probability. In particular, we use

$$f(\beta, I, m) = \left(1 - (1-\beta)^I\right)/g(m),$$

where $g(m)$ is either *linear*, $g(m) = m$, or $g(m) = m^2$ or $g(m) = \sqrt{m}$. The linear scenario should correspond to a decrease in risk in a hyperedge setting due to improved ventilation with a crude airflow dilution whereas $g(m) = \sqrt{m}$ corresponds to worse ventilation and $g(m) = m^2$ corresponds to both ventilation and volume impacts (i.e., big groups need both more air and more space/volume). To implement this, we simply run over all nodes and examine the hyperedges they are in. We then compute $f(\beta, I, m)$ for each hyperedge and infect the node with that probability. Otherwise, we implement the state transitions from the standard SIRS model.

We designed this model such that the epidemic model is closely related to a pairwise projected graph version of the hypergraph, where multiple edges would correspond with repeated possible infection attempts. The key difference is that we handle the airborne dilution *after* accounting for the increased infection probability due to multiple infected individuals.

4.2 Related Work on Epidemic Simulation

Existing work on epidemic spreading over hypergraphs often simulates epidemics using individual-level stochastic models or mean-field approximations of the continuous-time process [5,15,22]. While these approaches share similarities with discrete event simulations, there are some notable differences in the pairwise case regarding fine-scaled information and homogeneity assumptions [3,14,24]. For this reason, we make use of a discrete event simulator to more accurately model fine-scaled epidemic behavior. Thus where other efforts use a rate of infection in continuous time (and the ensuing non-linear term), we directly use probabilities for each discrete time step.

Another notable distinction in our approach is how we treat infections within hyperedges. Related research uses an infection rate that depends on the number of infected neighbors [5]. More precisely, the rate at which a node is infected due to a particular hyperedge is given by $f(\beta, I)$, which uses both an infection parameter β and the number of infected nodes in the hyperedge, I. The function $f(\beta, I, m)$ that we adopt varies based on the size of the hyperedge as well. We note that [15] uses a partitioned model that allows a different function for each value of m, but their analysis is based on a continuous-time formulation.

5 Results

The goal of our experiments is to show that the hypergraph structure changes a key macroscopic parameter for the epidemic. We first explain our parameters

(Sect. 5.1), then we illustrate an example epidemic trajectory in the large hyperedge case $\alpha = 2$ to illustrate how the normalization $g(m)$ impacts the behavior (Sect. 5.2, Fig. 4). Next, we show how the number of trailing infections changes among these models as we vary α (Fig. 5). For both of these, we consider how $g(m)$ impacts the results.

Since it is well known that both the average degree and value of λ_1 (the largest eigenvalue of the adjacency matrix) [8,21] are important parameters for an epidemic, we show both of these parameters for the weighted pairwise projection of the hypergraph. The graph projection was described in the preliminary section and as we noted, our hypergraph epidemic doesn't precisely correspond to a weighted pairwise epidemic. Nonetheless, they show relevant information on how much the *graph* portion of the hypergraph is contributing to epidemic forcing. We compare both weighted projected degree and λ_1 in Figs. 6, 7.

5.1 Parameter Setting and Simulation Details

In the interest of space, we investigate a single graph size, $n = 50000$ and $d = 2$. We use a log-normal distribution for r_v with mean neighborhood size $\log(3)$ and standard deviation 1. This produces a largest neighborhood of somewhere between 75 and 500. We set $\beta = 0.9, \gamma = 0.1, \delta = 0.01$. We also set $\theta = 5/1,000,000$ so that we expect one exogenous infection every four time steps. The epidemics are simulated for 3650 time steps.

Note that when we investigate distributions over α, we keep both the values of r_v and the coordinates x_v fixed as we vary the hypergraph constructed with α.

5.2 Epidemic Results

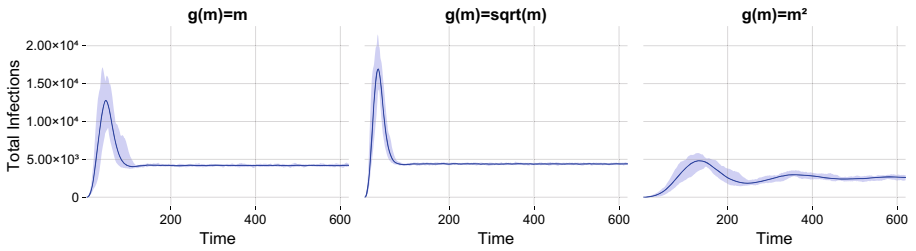

Fig. 4. From left to right the average (line) and extreme values (ribbon) from 25 SIRS epidemics by time for the specified $g(m)$ for the purely hyperedge case ($\alpha = 2$). The differences are due to changes in the influence of hyperedges in the spread.

Examples of epidemic trajectories are shown in Fig. 4. In this case, we generate one graph and compute 25 realizations of the SIRS epidemic. These figures

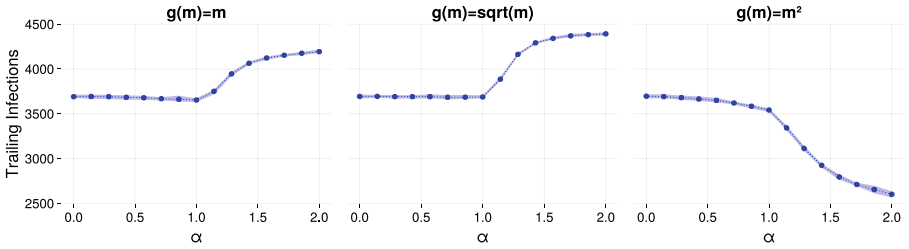

Fig. 5. Figure showing differences in the average trailing infections (y-axis) as we vary α (x-axis) for different normalization terms - $g(m)$. Markers indicate the average with the band indicating the min and max over 25 simulations for each value of α.

plot the total number of people in the infected state at each time step. Note that there is an initial spike as most of the network is infected, then this settles off to a steady state. This figure, for $\alpha = 2$, shows that in the large hyperedge regime, there is only a small difference between normalizing infection probabilities by $\sqrt{m}$ compared to m.

Next, we look at the average number of infections in the steady state regime in Fig. 5. To be precise, we take the last 1000 time steps of each epidemic trajectory and compute the average number of people in the infected state in each step over this time period. As we vary α, we can see a distinct effect, namely that average trailing infections are barely changed in the small hyperedge regime ($\alpha \leq 1$) for all the cases, whereas it grows distinctly for $g(m) = m$ and $g(m) = \sqrt{m}$ in the large hyperedge regime ($\alpha > 1$) and drops distinctly for $g(m) = m^2$. These all show clear impacts on the epidemic information in the large hyperedge regime.

5.3 Average Degrees and Largest Eigenvalues of the Projected Graph

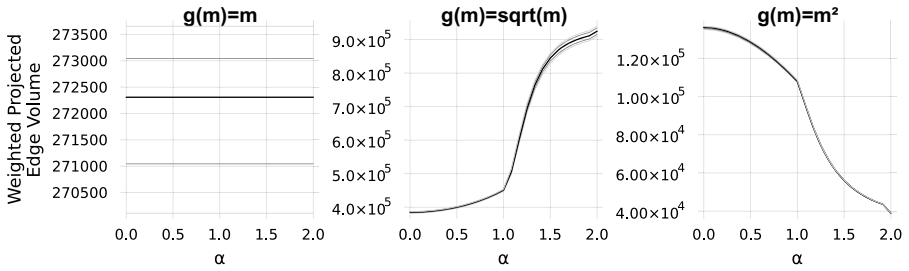

Fig. 6. From left to right, the projected degrees for the spatial hypergraph model generated using the same spatial data and degree information for 1) a linear projection, 2) a square root projection, and 3) a squared projection. Lines show the 10th, 25th, 50th, 75th, and 90th percentiles.

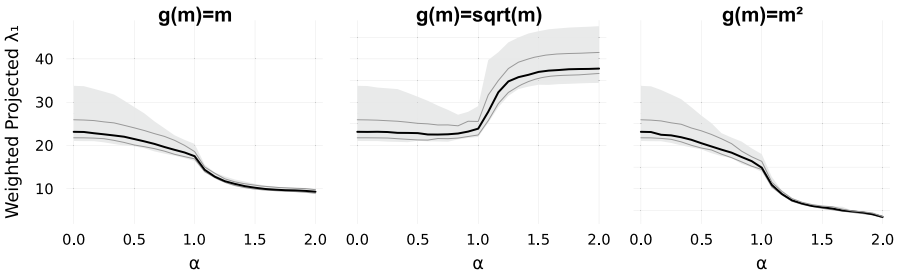

Fig. 7. From left to right, the dominant eigenvalue for the spatial hypergraph model generated using the same spatial data and degree information for 1) a linear projection, 2) a square root projection, and 3) a squared projection. Lines show the 10th, 50th, and 90th percentiles and the gray bands denote the max and min over 25 trials.

As previously mentioned, both the average degree and largest eigenvalue are known to be key features of epidemic spread in networks. To assess their impact on this experiment, we compute the weighted projected graph of these hypergraphs using the weighting function $g(m)$. Figure 6 shows the total degree volume of the projected graphs from these hypergraphs as we vary α. Recall that all graphs share the same spatial information and sampled degrees in this example. The degree-projected graph is constant for the linear normalization term $g(m) = m$ and increasing/decreasing for the square root/squared function as one would expect. In Fig. 7 we see the same information for the dominant eigenvalue of the weighted, projected adjacency matrix. All of these show trends that *are not* captured in the actual epidemic behavior. This shows that the difference in impact is directly due to the higher-order spreading patterns.

6 Discussion

There are two key contributions of this paper. The first is a flexible spatial hypergraph model. The second is a demonstration of how that model can be used to study higher-order impacts in epidemic spreading. Here, we see a clear case where the higher-order structure causes much higher epidemic prevalence than in the pairwise model. Pairwise projections are insufficient to explain this. To aid reproducibility, the code and data used in this study are publicly available at https://github.com/oeldaghar/spatial-hypergraph-epidemics.

We believe this demonstrates a clear case where higher-order spreading is relevant to epidemics – especially in the case of linear normalization ($g(m) = m$), although we acknowledge that our study currently only treats a limited parameter regime and does not yet explain a *mechanism* by which the average infections are higher. In the future, we plan to explore mechanisms underlying the difference.

In a different direction, we could make the epidemic simulation or the graph generation more realistic. For instance, we could use point distributions sampled

from population densities in a city. In terms of the epidemic spread, we could directly model the infection risk with shared air in terms of the relative risk indices [20]. We could also attempt to directly model potential mixing in large groups. Accuracy here is fraught as many parameters are extremely difficult to set. A more interesting direction is to explore the dynamics of viral shedding *within* a single infection wherein certain people are much more contagious at certain stages of their infection [11]. Finally, interventions can substantially change the picture of epidemic spread and how it interacts with network structure [12].

References

1. Ajelli, M., et al.: Comparing large-scale computational approaches to epidemic modeling: agent-based versus structured metapopulation models. BMC Infect. Dis. **10**, 1–13 (2010)
2. ASHRAE: Ventilation for Acceptable Indoor Air Quality, ANSI/ASHRAE standard 62.1–2019 edn. ASHRAE (2019). ANSI/ASHRAE 2019
3. Bansal, S., Grenfell, B.T., Meyers, L.A.: When individual behaviour matters: homogeneous and network models in epidemiology. J. R. Soc. Interface **4**(16), 879–891 (2007)
4. Bobrowski, O., Kahle, M.: Topology of random geometric complexes: a survey. J. Appl. Comput. Topol., 331–364 (2018). https://doi.org/10.1007/s41468-017-0010-0
5. Bodó, Á., Katona, G.Y., Simon, P.L.: SIS epidemic propagation on hypergraphs. Bull. Math. Biol. **78**, 713–735 (2016)
6. Bonato, A., Gleich, D.F., Kim, M., Mitsche, D., Prałat, P., Tian, Y., Young, S.J.: Dimensionality of social networks using motifs and eigenvalues. PLOS one **9**(9), e106052 (2014)
7. Bonato, A., Janssen, J., Prałat, P.: Geometric protean graphs. Internet Math. **8**(1–2), 2–28 (2012)
8. Chakrabarti, D., Wang, Y., Wang, C., Leskovec, J., Faloutsos, C.: Epidemic thresholds in real networks. ACM Trans. Info. Sys. Secur. **10**(4), 1–26 (2008)
9. Chang, S., et al.: Mobility network models of Covid-19 explain inequities and inform reopening. Nature **589**(7840), 82–87 (2021)
10. De Kergorlay, H.L., Higham, D.J.: Connectivity of random geometric hypergraphs. Entropy **25**(11), 1555 (2023)
11. Dixit, A.K., Espinoza, B., Qiu, Z., Vullikanti, A., Marathe, M.V.: Airborne disease transmission during indoor gatherings over multiple time scales: Modeling framework and policy implications. Proc. Natl. Acad. Sci. **120**(16), e2216948120 (2023)
12. Eldaghar, O., Mahoney, M.W., Gleich, D.F.: Multi-scale local network structure critically impacts epidemic spread and interventions. arXiv:2312.17351 (2023)
13. Ester, M., Kriegel, H.P., Sander, J., Xu, X., et al.: A density-based algorithm for discovering clusters in large spatial databases with noise. In: KDD, pp. 226–231 (1996)
14. Großmann, G., Backenköhler, M., Wolf, V.: Heterogeneity matters: Contact structure and individual variation shape epidemic dynamics. PLOS One **16**(7), e0250050 (2021)
15. Higham, D.J., De Kergorlay, H.L.: Epidemics on hypergraphs: spectral thresholds for extinction. Proc. Royal Soc. A **477**(2252), 20210232 (2021)

16. Huang, Y., Gleich, D.F., Veldt, N.: Densest subHyperGraph: negative supermodular functions and strongly localized methods. In: TheWebConf, pp. 881–892 (2024)
17. Kahle, M.: Random geometric complexes. Disc. Comput. Geom. **45**, 553–573 (2011)
18. Lu, J., et al.: Covid-19 outbreak associated with air conditioning in restaurant, Guangzhou, China, 2020. Emerg. Infect. Dis. **26**(7), 1628–1631 (2020)
19. Lunagómez, S., Mukherjee, S., Wolpert, R.L., Airoldi, E.M.: Geometric representations of random hypergraphs. J. Am. Stat. Assoc. **112**(517), 363–383 (2017)
20. Peng, Z., Rojas, A.P., Kropff, E., et al.: Practical indicators for risk of airborne transmission in shared indoor environments and their application to covid-19 outbreaks. Environ. Sci. Technol. **56**(2), 1125–1137 (2022)
21. Prakash, B.A., Chakrabarti, D., Faloutsos, M., Valler, N., Faloutsos, C.: Threshold conditions for arbitrary cascade models on arbitrary networks. In: 2011 IEEE 11th ICDM, vol. 14, p. 537–546. IEEE (2011)
22. Suo, Q., Guo, J.L., Shen, A.Z.: Information spreading dynamics in hypernetworks. Phys. A **495**, 475–487 (2018)
23. Turnbull, K., Lunagómez, S., Nemeth, C., Airoldi, E.: Latent space modeling of hypergraph data. J. Am. Stat. Assoc. **119**, 2634–2646 (2023). https://doi.org/10.1080/01621459.2023.2270750
24. Volz, E.M., Miller, J.C., Galvani, A., Ancel Meyers, L.: Effects of heterogeneous and clustered contact patterns on infectious disease dynamics. PLoS Comput. Biol. **7**(6), e1002042 (2011)